Transport properties of anyons in random topological environments

V. Zatloukal,[1] L. Lehman,[2] S. Singh,[2] J. K. Pachos,[3] and G. K. Brennen[2,3]

[1]*Faculty of Nuclear Sciences and Physical Engineering, Czech Technical University in Prague, Břehová 7, 115 19 Praha 1, Czech Republic*
[2]*Centre for Engineered Quantum Systems, Department of Physics and Astronomy, Macquarie University, North Ryde,*
New South Wales 2109, Australia
[3]*School of Physics and Astronomy, University of Leeds, Leeds LS2 9JT, United Kingdom*

The quasi-one-dimensional transport of Abelian and non-Abelian anyons is studied in the presence of a random topological background. In particular, we consider the quantum walk of an anyon that braids around islands of randomly filled static anyons of the same type. Two distinct behaviors are identified. We analytically demonstrate that all types of Abelian anyons localize purely due to the statistical phases induced by their random anyonic environment. In contrast, we numerically show that non-Abelian Ising anyons do not localize. This is due to their entanglement with the anyonic environment, which effectively induces dephasing. Our study demonstrates that localization properties strongly depend on nonlocal topological interactions, and it provides a clear distinction in the transport properties of Abelian and non-Abelian anyons.

PACS number(s): 05.30.Pr, 03.65.Vf, 05.40.Fb

I. INTRODUCTION

In systems with physics constrained to two dimensions, pointlike particles called anyons, which have more general statistics than bosons or fermions, can occur [1]. Beyond the mere possibility of their existence, they were found to be a good description for low-lying quasiparticle excitations of fractional quantum Hall (FQH) systems and Majorana edge modes of nanowires, and they exactly describe excitations in various strongly correlated two-dimensional spin-lattice models [2]. Recently, there has been experimental progress in the preparation and control of systems capable of exhibiting topological order with the goal of observing anyonic statistics [3,4]. This research is further motivated by the discovery that braiding some types of non-Abelian anyons provides for naturally fault-tolerant quantum computing [2,5]. As we are not yet able to manipulate anyons individually, it would be beneficial to reveal their exotic braiding properties on a macroscopic scale. In particular, we are interested in the transport properties of anyons and their possible localization, which can have direct observable consequences.

Transport properties of anyons in uniform backgrounds were studied in [6] using a discrete-time quantum walk. The dispersion of the walker was found to be quadratic for Abelian anyons, as in the usual quantum walk [7], while for non-Abelian anyons it has been shown to be asymptotically linear [8,9], just like in classical random walks. The essential reason is that entanglement resulting from braiding non-Abelian anyons is sufficient to suppress the quantum correlations responsible for the quadratic speedup.

In this work, we investigate the role of disorder in the propagation of both Abelian and non-Abelian anyons. It has been known for more than five decades that randomized local potentials can suppress diffusion of quantum particles, a phenomenon known as Anderson localization [10]. This mechanism is based on randomization of phases that correspond to individual particle histories and consequent destructive interference. Here we consider a discrete-time anyonic quantum walk in a disordered topological background. In particular, we consider a walker that braids around islands canonically arranged on a line, where the number of static anyons at a given island assumes a random value. For the Abelian anyons this causes the walker to acquire random *discrete* phases, which, as we demonstrate, leads to localization. For the non-Abelian ones the Hilbert space grows exponentially with the number of anyons and hence the length of the walk. As this makes long-time exact numerics prohibitive, we introduce an anyonic Hubbard model and use an anyonic matrix product state evolution to efficiently model continuous-time transport. The result is that Ising non-Abelian anyons do not localize. These generic behaviors provide a very clear distinction in the transport properties of Abelian and non-Abelian anyons.

II. THE DISCRETE-TIME MODEL

Our setup consists of n "islands" canonically ordered on the surface and labeled by index s, as shown in Fig. 1. The sth island is occupied by m_s static anyons ($m_s \geqslant 0$), and the configuration, represented by vector $\vec{m} = (m_1, \ldots, m_n)$, is supposed to be fixed during the course of the walk. Anyons are labeled within an island from left to right by an index $i_s = 1, \ldots, m_s$. The mobile *walker* anyon hops between neighboring sites winding counterclockwise around the islands. Hence our system is quasi-one-dimensional. We also denote a possible walker's spatial positions by s, with the convention that position s lies between islands $s-1$ and s, as shown in Fig. 1. The distance between sites is set to unity, although for purely topological interactions the distance scale is irrelevant. Hopping direction is controlled by the coin state: $|0\rangle$ moves the walker to the left, and $|1\rangle$ moves the walker to the right. The total Hilbert space decomposes as $\mathcal{H} = \mathcal{H}_{\text{space}} \otimes \mathcal{H}_{\text{coin}} \otimes \mathcal{H}_{\text{fusion}}$, where $\mathcal{H}_{\text{space}} = \text{span}_{\mathbb{C}}\{|s\rangle\}_{s=1}^n$, $\mathcal{H}_{\text{coin}} = \text{span}_{\mathbb{C}}\{|0\rangle, |1\rangle\}$, and $\mathcal{H}_{\text{fusion}}$ enumerates all distinct measurement outcomes of topological charge when pairs of anyons are fused together [5].

One step of the walk is defined as a composition of two unitary operations, $W = TU$, where $U = \frac{1}{\sqrt{2}}\begin{pmatrix} 1 & 1 \\ 1 & -1 \end{pmatrix}$ acts in the coin space and T is a conditional braiding operator which
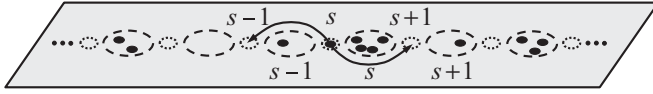
FIG. 1. The quasi-one-dimensional quantum walk of an anyon braiding counterclockwise around islands filled with a random number of static anyons of the same type. The islands, denoted with dashed circles, are canonically arranged on the line. The possible positions of the walker are denoted by dotted circles placed in between the islands.

moves the walker left or right depending on the coin state:

$$T = \sum_{s=1}^{n} |s-1\rangle\langle s| \otimes |0\rangle\langle 0| \otimes \hat{b}_{s-1}$$
$$+ |s+1\rangle\langle s| \otimes |1\rangle\langle 1| \otimes \check{b}_s, \quad (1)$$

where $\hat{b}_s = b_{s,1}\cdots b_{s,m_s}$, $\check{b}_s = b_{s,m_s}\cdots b_{s,1}$, and $\hat{b}_s = \check{b}_s = 1$ if $m_s = 0$. The operators $\{b_{s,i_s}\}$, acting on the fusion space $\mathcal{H}_{\text{fusion}}$, form a unitary representation of the r-strand braid group, $r = 1 + \sum_{s=1}^{n} m_s$, which reflects the type of anyons we choose. To make T unitary, we assume periodic boundary conditions $(|0\rangle_{\text{space}} = |n\rangle_{\text{space}})$ but will be concerned with walks satisfying $t < n/2$, where t is the number of steps, so that winding around the surface is not an issue. Note that this model is *chiral* because only counterclockwise braids are considered. This is in close analogy to edge states in FQH liquids where the breaking of time-reversal symmetry in the bulk results in a net current in one direction at the edge. Below we also consider a continuous-time model where braiding is allowed in both directions. The qualitative behavior of the variance in this model is similar to the chiral discrete-time model.

Let the system's initial state be $|\Psi(0)\rangle = |s_0\rangle|c_0\rangle|\Phi_0\rangle$, where $s_0 = \lceil n/2 \rceil$ is the initial position of the walker, $c_0 = 0$ denotes the initial state of the coin, and Φ_0 depends on the initial state of the anyons. After t iterations of the one-step operator W, the state becomes $|\Psi(t)\rangle = W^t|\Psi(0)\rangle$, a superposition over all coin histories $\vec{a} \in \{0,1\}^{\otimes t}$, weighted by appropriate phase factors. The reduced state of the spatial degree of freedom of the walker is

$$\rho_{\text{space}}(t) = \text{tr}_{\text{coin}}\text{tr}_{\text{fusion}}|\Psi(t)\rangle\langle\Psi(t)|$$
$$= \sum_{\vec{a},\vec{a}'} \text{tr}\mathcal{U}_{\vec{a}\vec{a}'}\text{tr}\mathcal{Y}_{\vec{a}\vec{a}'}|s_{\vec{a}}\rangle\langle s_{\vec{a}'}|, \quad (2)$$

where $s_{\vec{a}} = s_0 + \sum_{k=1}^{t}(2a_k - 1)$ is the walker's final position corresponding to the coin history $\vec{a} = (a_1, \dots, a_t)$; $\text{tr}\mathcal{U}_{\vec{a}\vec{a}'} = \frac{1}{2^t}(-1)^{z(\vec{a},\vec{a}')}$, with $z(\vec{a},\vec{a}') \equiv \sum_{k=1}^{t-1}(a_k a_{k+1} + a'_k a'_{k+1})$, is a partial trace over the coin degree of freedom (DOF); and $\mathcal{Y}_{\vec{a}\vec{a}'} = B_{\vec{a}}|\Phi_0\rangle\langle\Phi_0|B_{\vec{a}'}^\dagger$ acts in the fusion space. The braid word $B_{\vec{a}}$ can be constructed recursively from a given coin history $\vec{a}$:

$$B_{\vec{a}^{(k+1)}} = \begin{cases} \hat{b}_{s_{\vec{a}^{(k)}}-1}B_{\vec{a}^{(k)}} & \text{if} \quad a_{k+1} = 0, \\ \check{b}_{s_{\vec{a}^{(k)}}}B_{\vec{a}^{(k)}} & \text{if} \quad a_{k+1} = 1, \end{cases} \quad (3)$$

where $\vec{a}^{(k)} = (a_1, \dots, a_k)$ is a truncation of $\vec{a}$, $s_{\vec{a}^{(0)}} = s_0$, and $B_{\vec{a}^{(0)}} = 1$.
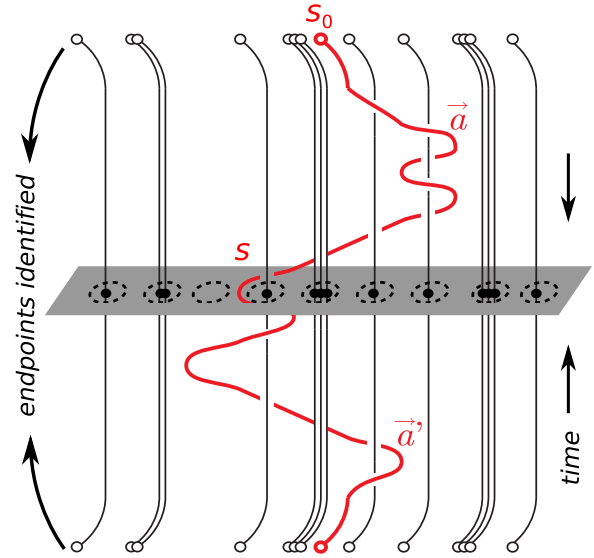

FIG. 2. (Color online) World line of the mobile anyon constructed from a pair of paths $(\vec{a},\vec{a}') \rightsquigarrow s$. Together with the world lines of the static anyons, they give rise to the link $L_{\vec{a}\vec{a}'}$ via the Markov closure of the braid word $B_{\vec{a}'}^\dagger B_{\vec{a}}$, which identifies the corresponding end points. (All the particle world lines are assumed to have a common orientation.) Linking numbers $\ell_s(\vec{a},\vec{a}')$ as defined in Fig. 3 are easily read off, e.g., $\ell_s = -1$, $\ell_{s+1} = 0$, etc.

The spatial distribution of the walker after t steps is given by diagonal elements of the reduced density matrix,

$$p_{\vec{m}}(s,t) \equiv \langle s|\rho_{\text{space}}(t)|s\rangle = \frac{1}{2^t}\sum_{(\vec{a},\vec{a}')\rightsquigarrow s}(-1)^{z(\vec{a},\vec{a}')}\text{tr}\mathcal{Y}_{\vec{a}\vec{a}'}, \quad (4)$$

where "$(\vec{a},\vec{a}') \rightsquigarrow s$" denotes the set of pairs of paths $(\vec{a},\vec{a}')$ satisfying $a_t = a'_t$ and $s_{\vec{a}} = s_{\vec{a}'} = s$ (see Fig. 2). The subscript $\vec{m}$ indicates a fixed island occupation configuration. Variance of the probability distribution $p_{\vec{m}}(s,t)$ is defined in the usual way: $\sigma_{\vec{m}}^2(t) = \sum_s p_{\vec{m}}(s,t)s^2 - [\sum_s p_{\vec{m}}(s,t)s]^2$.

In studies of transport phenomena in disordered environments, one is interested in quantities that result from averaging over all random background configurations. We shall assume that the island occupation numbers m_s are independent and identically distributed random variables with distribution $W(m_s)$. The probability of occurrence of a configuration $\vec{m}$ is then simply $W_{\vec{m}} = \prod_{s=1}^{n} W(m_s)$, and we denote the configuration average of a quantity $Q_{\vec{m}}$ by $\langle\langle Q \rangle\rangle \equiv \sum_{\vec{m}} W_{\vec{m}}Q_{\vec{m}}$. The average position distribution after a t-step walk is given by

$$\langle\langle p(s,t) \rangle\rangle = \frac{1}{2^t}\sum_{(\vec{a},\vec{a}')\rightsquigarrow s}(-1)^{z(\vec{a},\vec{a}')}\langle\langle\text{tr}\mathcal{Y}_{\vec{a}\vec{a}'}\rangle\rangle. \quad (5)$$

The topological quantity $\langle\langle\text{tr}\mathcal{Y}_{\vec{a}\vec{a}'}\rangle\rangle$, which depends on particle statistics, governs the transport of an anyonic walker in a random background.

III. ABELIAN ANYONS

For Abelian anyons the braid generators $\{b_{s,i_s}\}$ are all equal to $e^{i\phi}$. We assume the anyonic exchange angle is $\phi = \pm\frac{\pi}{N}$, $N \in \mathbb{N}$. The fusion space is one-dimensional, $\mathcal{H}_{\text{fusion}} \simeq \mathbb{C}$, and we can choose $|\Phi_0\rangle$ arbitrarily. Upon introducing the
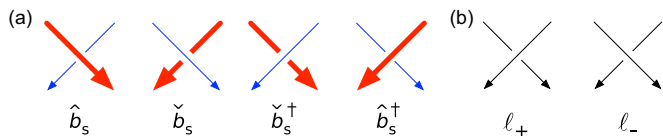
FIG. 3. (Color online) (a) The linking number between the walker's component (thin blue arrows) and the world line of an island s (thick red arrows), which collects all components of the island's static anyons, is determined by the relative number of four types of crossings $\ell_s = \frac{-\#\hat{b}_s - \#\check{b}_s + \#\hat{b}_s^\dagger + \#\check{b}_s^\dagger}{2}$. (b) The writhe of a link is the difference of the number of positive crossings and negative crossings: $w(L) = \ell_+ - \ell_-$.

linking numbers $\ell_s(\vec{a}, \vec{a}') = \frac{-\#(\hat{b}_s \text{ and } \check{b}_s \text{ in } B_{\vec{a}}) + \#(\hat{b}_s^\dagger \text{ and } \check{b}_s^\dagger \text{ in } B_{\vec{a}'}^\dagger)}{2}$, which count the number of times the walker's trajectory $(\vec{a}, \vec{a}')$ winds around an island s [see Figs. 2 and 3(a)], tr$\mathcal{Y}_{\vec{a}\vec{a}'}$ reduces to $\prod_{s=1}^n e^{\mp i 2 \frac{\pi}{N} m_s \ell_s(\vec{a}, \vec{a}')}$.

For simplicity we consider a uniform occupation distribution: $W(m) = 1/N$ for $0 \leqslant m \leqslant N - 1$. Then the average position distribution of the walker after t steps, $\langle\langle p^{(\pm \frac{\pi}{N})}(s,t)\rangle\rangle$, is given by (5) with

$$\langle\langle \text{tr} \mathcal{Y}_{\vec{a}\vec{a}'}^{(\pm \frac{\pi}{N})} \rangle\rangle = \prod_{s=1}^n \delta_{0, \ell_s(\vec{a}, \vec{a}') \bmod N}, \qquad (6)$$

where $\delta_{i,j}$ is the Kronecker symbol.

Localization of the distribution can be proven analytically by mapping the model to a variation of the one-dimensional multiple scattering model presented in [11]. (We base the correspondence between the two on physical intuition rather than mathematical rigor.) In that work, scatterers are arranged in line with *continuous* random distances between neighbors. Incoming light undergoes a series of scattering events and eventually localizes due to the randomness in phases that individual trajectories accumulate during their passage between consecutive scatterers. In our variation the braiding phases, accumulated when traversing each island populated with a random numbers of anyons, take values in the *discrete* set $\{\frac{\pi m}{N}, 0 \leqslant m \leqslant N - 1\}$, and reflection and transmission coefficients of the scatterers are identified with the entries of the coin operator.

The scattering model is described by Fig. 4. A monochromatic wave incident from the left scatters on a series of scatterers characterized by reflection and transmission coefficients from the left (r_j, t_j) and from the right (r_j', t_j'). The distance between two successive scatterers j and $j + 1$ is random, such
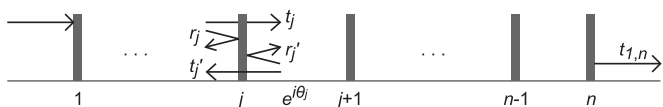

FIG. 4. In the multiple-scattering model, the wave approaches (from the left) a series of n scatterers and is transmitted with the amplitude $t_{1,n}$. The scatterers are arranged in a line with random distances between neighbors. Hence the phases $e^{i\theta_j}$ that the wave acquires while traveling from scatterer j to scatterer $j + 1$ are also random. The complex quantities r_j, t_j and r_j', t_j' are the reflection and transmission amplitudes for the wave impinging from the left and from the right, respectively.

that the phase that the wave acquires when traveling between j and $j + 1$ is $e^{i\theta_j}$.

Amplitude of transmission from the "left of scatterer 1" to the "right of scatterer n" and by $r_{1,n}'$ the reflection amplitude from the block "1 to n" when approaching from the right. $t_{1,n}$ can be expressed by the series

$$t_{1,n} = t_{1,n-1} e^{i\theta_{n-1}} \sum_{k=0}^\infty \left(r_n e^{i\theta_{n-1}} r_{1,n-1}' e^{i\theta_{n-1}} \right)^k t_n$$

$$= \frac{t_{1,n-1} e^{i\theta_{n-1}} t_n}{1 - r_n r_{1,n-1}' e^{i2\theta_{n-1}}}. \qquad (7)$$

The corresponding transmission probability and its logarithm are given by

$$|t_{1,n}|^2 = \frac{|t_{1,n-1}|^2 |t_n|^2}{|1 - r_n r_{1,n-1}' e^{i2\theta_{n-1}}|^2}, \qquad (8)$$

$$\ln |t_{1,n}|^2 = \ln |t_{1,n-1}|^2 + \ln |t_n|^2 - \ln |1 - r_n r_{1,n-1}' e^{i2\theta_{n-1}}|^2. \qquad (9)$$

The reflection and transmission amplitudes $t_{1,n}$, $r_{1,n}'$ are random variables that depend on the configuration of scatterers $1, \ldots, n$, i.e., on the angles $\theta_1, \ldots, \theta_{n-1}$. We assume that θ_j's are identically distributed independent random variables with a uniform distribution over the discrete set $\{\frac{\pi}{N} m \mid m = 0, \ldots, N - 1\}$ ($\frac{\pi}{N}$ will be identified with the anyonic exchange angle ϕ) [12]. We shall denote by $\langle\langle(\cdots)\rangle\rangle$ the statistical average over the angles $\theta_1, \ldots, \theta_{n-1}$, i.e.,

$$\langle\langle(\cdots)\rangle\rangle \equiv \sum_{m_1=0}^{N-1} \frac{1}{N} \cdots \sum_{m_{n-1}=0}^{N-1} \frac{1}{N}(\cdots). \qquad (10)$$

Averaging (9) leads to

$$\langle\langle \ln |t_{1,n}|^2 \rangle\rangle = \langle\langle \ln |t_{1,n-1}|^2 \rangle\rangle + \ln |t_n|^2$$
$$- \langle\langle \ln |1 - r_n r_{1,n-1}' e^{i2\theta_{n-1}}|^2 \rangle\rangle. \qquad (11)$$

We shall now assume that $t_j = t, r_j = r$ for all j. On the level of the Abelian anyonic quantum walk, this corresponds to a spatially independent coin. Bounds on the value of $\langle\langle \ln |t_{1,n}|^2 \rangle\rangle$ are computed in Appendix A1 [see Eq. (A7)]. Exponentiating the resulting bounds results in

$$\exp\langle\langle \ln |t_{1,n}|^2 \rangle\rangle \leqslant (1 - |r|^N)^{\frac{2}{N}} e^{-n[\ln(1-|r|^N)^{\frac{2}{N}} - \ln |t|^2]},$$

$$\exp\langle\langle \ln |t_{1,n}|^2 \rangle\rangle \geqslant (1 + |r|^N)^{\frac{2}{N}} e^{-n[\ln(1+|r|^N)^{\frac{2}{N}} - \ln |t|^2]}. \qquad (12)$$

Estimates of the localization length ξ_{loc} follow

$$\frac{1}{\ln(1 + |r|^N)^{\frac{2}{N}} - \ln |t|^2} \leqslant \xi_{\text{loc}} \leqslant \frac{1}{\ln(1 - |r|^N)^{\frac{2}{N}} - \ln |t|^2}, \qquad (13)$$

where the anyonic statistical angle $\phi = \frac{\pi}{N}$. For $N \to \infty$ we have $\xi_{\text{loc}} \to -\frac{1}{\ln |t|^2}$.

For the upper bound in (13) to make sense, $-\ln |t|^2 + \frac{1}{N} \ln(1 - |r|^N)^2$ has to be a positive number. This leads to the condition $|t|^2 < (1 - |r|^N)^{\frac{2}{N}}$, i.e.,
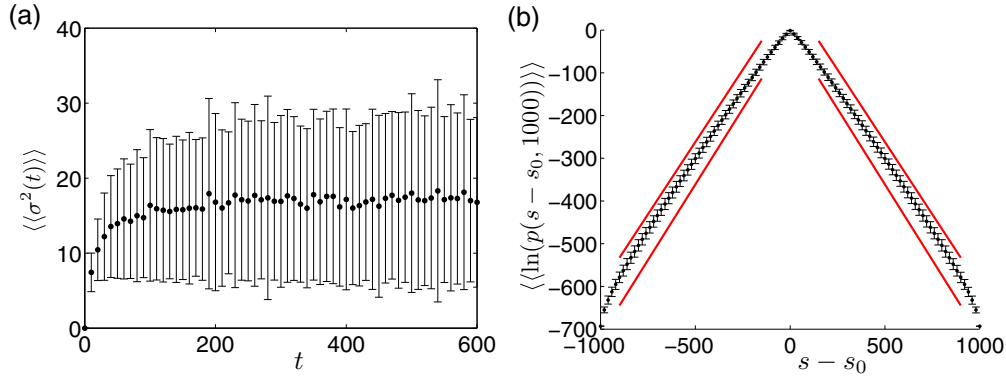
$$|t|^N + |r|^N < 1. \qquad (14)$$

FIG. 5. (Color online) Numerical results for localization of Abelian anyons. The exchange statistics is $\phi = \frac{\pi}{8}$, and the statistics is averaged over a random background of island occupations where the distribution in each is uniform over $m_s \in \{0, \ldots, 7\}$. (a) Average variance as a function of time t for up to 600 time steps. The averages are taken over at least 500 charge configurations. (For clarity, only every tenth step is plotted.) (b) Average of the logarithm of probability distribution at time step $t = 1000$, taken over 10 000 charge configurations. Red lines correspond to bounds for the localization length given in Eq. (16). In both (a) and (b), the error bars are given by the standard deviation.

Since $|t|^2 + |r|^2 = 1$ (with $|t|, |r| < 1$), the latter is satisfied for $N > 2$.

The case $N = 1$ corresponds to fermions, which are known not to localize (their exchange statistics does not induce any interference effects). The marginal case $N = 2$ corresponds to *semions* ($\phi = \pi/2$), but we are unable to determine their localization within this method. However, numerics for an analogous model involving continuous-time hopping of semions on a ladder support localization [13].

To establish a connection between this scattering model and the Abelian anyonic quantum walk with the coin $U = \frac{1}{\sqrt{2}} \begin{pmatrix} 1 & 1 \\ 1 & -1 \end{pmatrix}$, we define

$$t = -\frac{1}{\sqrt{2}}, \quad t' = \frac{1}{\sqrt{2}}, \quad r = \frac{1}{\sqrt{2}}, \quad r' = \frac{1}{\sqrt{2}}. \quad (15)$$

The localization length estimate for $N = 8$ ($\frac{\pi}{8}$-anyons) is

$$1.412 \leqslant \xi_{\text{loc}} \leqslant 1.477. \quad (16)$$

Let us stress that we investigated the stationary state of a wave after infinitely many scattering events. This corresponds to the infinite-time asymptotic behavior of the anyonic quantum walk.

The result (13) works for any $N > 2$, thus extending prior work which assumed a continuum of values in the scattering length, i.e., $N \to \infty$ [14,15], or rationally independent values [16]. Figure 5 shows numerical results for the case $N = 8$. This case describes statistics for Abelian excitations in the $U(1)_8$ theory for the $\nu = 1/2$ fractional quantum Hall state where charge $2e$ electron pairs form an effective $\nu = 1/8$ bosonic Laughlin state [17], and it is also relevant to the non-Abelian case described below. The variance approaches a constant value, and the asymptotic position distribution assumes a characteristic exponential shape, $\langle\langle p^{(\pm\frac{\pi}{N})}(s, t \to \infty)\rangle\rangle \sim e^{-\frac{|s - s_0|}{\xi_{\text{loc}}}}$, with the localization length $\xi_{\text{loc}} \doteq 1.44$. This is a clear manifestation of the Anderson localization of Abelian anyons.

IV. ISING NON-ABELIAN ANYONS

We consider the Ising model of non-Abelian anyons. There are three kinds of particles in this model: vacuum, fermion, and non-Abelian anyon. In analogy with the notation in [8], the initial fusion state $|\Phi_0\rangle$ describes the vacuum configuration of pairs of anyons with half the members braided to the right. Here they randomly populate islands (except for the walker) to form a disordered background configuration $\vec{m}$. The braid generators $\{b_{s, i_s}\}$ are now unitary matrices, the dimension of which grows as $d^{|\vec{m}|}$, where $|\vec{m}| \equiv \sum_{s=1}^{n} m_s$ and $d = \sqrt{2}$ is the *quantum dimension* of Ising anyons. This exponential increase in the Hilbert space dimension as well as the nonlocal character of the total braiding makes the evolution distinct from other quasi-one-dimensional systems.

The trace over the fusion degree of freedom can be related to the Kauffman bracket polynomial $\langle L_{\vec{a}\vec{a}'}\rangle$ [18] of a link $L_{\vec{a}\vec{a}'}$ (see Fig. 2), which arises from the Markov closure of the braid word $B_{\vec{a}'}^{\dagger} B_{\vec{a}}$ [6,8,19]. This link corresponds to the world lines (strands) of all the anyons. Moreover, $\langle L_{\vec{a}\vec{a}'}\rangle$ can be expressed in terms of the Jones polynomial $V_{L_{\vec{a}\vec{a}'}}(q)$ [20]. Altogether,

$$\text{tr}\mathcal{Y}_{\vec{a}\vec{a}'} = \frac{\langle L_{\vec{a}\vec{a}'}\rangle(q^{-1/4})}{d^{|\vec{m}|}} = \frac{(-q^{-3/4})^{w(L_{\vec{a}\vec{a}'})} V_{L_{\vec{a}\vec{a}'}}(q)}{d^{|\vec{m}|}}, \quad (17)$$

where the *writhe* $w(L_{\vec{a}\vec{a}'}) = 2 \sum_{s=1}^{n} m_s \ell_s(\vec{a}, \vec{a}')$ is the difference between the number of positive and negative crossings of the anyonic world lines [see Fig. 3(b)]. For Ising model anyons, which correspond to spin-1/2 irreps of the quantum group $SU(2)_2$, we have specifically $q = i$. Note there are some differences in the braid matrices for the Ising model and $SU(2)_2$ models, but they do not affect the results herein, as we discuss at the end of this section.

The Jones polynomial $V_{L_{\vec{a}\vec{a}'}}(i)$ for the links relevant to the quantum walk can be further simplified in terms of simple topological characteristics, the Arf invariant, through [21]

$$V_{L_{\vec{a}\vec{a}'}}(i) = \sqrt{2}^{|\vec{m}|} (-1)^{\text{Arf}(L_{\vec{a}\vec{a}'})} \prod_{\substack{s=1 \\ m_s > 0}}^{n} \widetilde{\ell}_s, \quad (18)$$

where $\widetilde{\ell}_s \equiv \delta_{0,\ell_s \bmod 2}$. The product in the last expression is equal to 1 only if the link $L_{\bar{a}\bar{a}'}$ is *proper*, i.e., the sum of the pairwise linking numbers is even. Furthermore, when the link is *totally proper*, i.e., all pairs of components have an even linking number, and there is no self-linking, then [22]

$$\text{Arf}(L_{\bar{a}\bar{a}'}) = \sum_{s=1}^{n} m_s c_2(s) + \sum_{1 \leqslant s' < s'' \leqslant n} m_{s'} m_{s''} \tau(s', s''), \quad (19)$$

where $c_2(s)$ is the cubic coefficient in the *Conway polynomial* of the two-component sublink of $L_{\bar{a}\bar{a}'}$ consisting of strands corresponding to the walker and island s and $\tau(s', s'')$ is the Milnor triple invariant, which counts the number of Borromean rings (three braided loops that disentangle if just one is removed) between the walker strand and strands s' and s''. Note there is no self-linking because the links represent world lines of the anyons, which only move forward in time. In Ref. [8] it was shown that for a uniformly filled background, for all the links that contribute to the spatial probability distribution, properness implies total properness. For nonuniform filling the same is true for the simple reason that paths that have even linking between the walker and one island anyon will then have multiple pairwise linking when the island has multiple occupancy.

Inserting (18) and (19) into the expression for the fusion space trace [Eq. (17)], we obtain

$$\text{tr}\mathcal{Y}_{\bar{a}\bar{a}'} = (-i^{-\frac{3}{4}})^{w(L_{\bar{a}\bar{a}'})} (-1)^{arf(L_{\bar{a}\bar{a}'})} \prod_{\substack{s=1 \\ m_s > 0}}^{n} \widetilde{\ell}_s$$

$$= (-1)^{\sum_{s' < s''} m_{s'} m_{s''} \tau(s', s'')}$$

$$\times \prod_{\substack{s=1 \\ m_s > 0}}^{n} \widetilde{\ell}_s (i)^{\frac{\ell_s}{2} m_s} (-1)^{m_s c_2(s)}. \quad (20)$$

For islands s such that $m_s > 0$ and $\widetilde{\ell}_s = 1$, i.e., $\frac{\ell_s}{2} \in \mathbb{Z}$, we can use a result of [8] and simplify

$$c_2(s) = \frac{\ell_s}{6}(\ell_s^2 - 1) = \frac{\ell_s}{2} \frac{1}{3} \left[4 \left(\frac{\ell_s}{2} \right)^2 - 1 \right] \stackrel{\bmod 2}{=} \frac{\ell_s}{2}. \quad (21)$$

Hence, our final result for $\text{tr}\mathcal{Y}_{\bar{a}\bar{a}'}$ reads

$$\text{tr}\mathcal{Y}_{\bar{a}\bar{a}'} = \prod_{\substack{s=1 \\ m_s > 0}}^{n} \widetilde{\ell}_s (-i)^{\frac{\ell_s}{2} m_s} \prod_{1 \leqslant s' < s'' \leqslant n} (-1)^{m_{s'} m_{s''} \tau(s', s'')}. \quad (22)$$

For uniform background configuration we recover the case studied in [8].

To illustrate the role of disorder in a non-Abelian anyonic quantum walk, we choose uniform island occupation probabilities. As (22) is for $m_s > 0$ 4 periodic in m_s we take $W(m) = 1/4$ for $1 \leqslant m \leqslant 4$ and $W(m) = 0$ otherwise [23]. The average trace over the fusion space for Ising model anyons

is calculated as

$$\langle\langle \text{tr}\mathcal{Y}_{\bar{a}\bar{a}'} \rangle\rangle = \sum_{\vec{m} \in \{1,\ldots,4\}^n} \frac{1}{4^n} \prod_{s=1}^{n} \widetilde{\ell}_s (-i)^{\frac{\ell_s}{2} m_s}$$

$$\times \prod_{1 \leqslant s' < s'' \leqslant n} (-1)^{m_{s'} m_{s''} \tau(s', s'')}. \quad (23)$$

We observe the following:

$$\langle\langle \text{tr}\mathcal{Y}_{\bar{a}\bar{a}'} \rangle\rangle = \left[\prod_{s=1}^{n} \widetilde{\ell}_s \right] \frac{1}{4^{n-1}} \sum_{\vec{m} \in \{1,\ldots,4\}^{n-1}} \prod_{s=1}^{n-1} (-i)^{\frac{\ell_s}{2} m_s}$$

$$\times \prod_{1 \leqslant s' < s'' \leqslant n-1} (-1)^{m_{s'} m_{s''} \tau(s', s'')}$$

$$\times \frac{1}{4} \sum_{m_n=1}^{4} \left[(-i)^{\frac{\ell_n}{2}} \right]^{m_n} \left[\prod_{s'=1}^{n-1} (-1)^{m_{s'} \tau(s', n)} \right]^{m_n}$$

$$= \cdots \times \begin{cases} 1 & \text{if } (-i)^{\frac{\ell_n}{2}}(-1)^{\sum_{s'=1}^{n-1} m_{s'} \tau(s', n)} = 1, \\ 0 & \text{otherwise.} \end{cases}$$

$$(24)$$

Hence, $\langle\langle \text{tr}\mathcal{Y}_{\bar{a}\bar{a}'} \rangle\rangle = 0$ whenever $\ell_n \neq 0 \bmod 4$ [i.e., when $(-i)^{\frac{\ell_n}{2}}$ is not a real number]. Furthermore, if $\ell_n = 4 \bmod 8$, then $\tau(s', n) = 0$ for all $r = 1, \ldots, n-1$ [24], and therefore $(-1)^{\frac{\ell_n}{4}}(-1)^{\sum_{s'=1}^{n-1} m_{s'} \tau(s', n)} = -1$. Hence, $\langle\langle \text{tr}\mathcal{Y}_{\bar{a}\bar{a}'} \rangle\rangle = 0$ whenever $\ell_n \neq 0 \bmod 8$. By the same reasoning, analogous conditions on ℓ_s hold for all islands $s = 1, \ldots, n$.

Let us define $\widetilde{\widetilde{\ell}}_s \equiv \delta_{0,\ell_s \bmod 8}$. We have

$$\langle\langle \text{tr}\mathcal{Y}_{\bar{a}\bar{a}'} \rangle\rangle = \prod_{s=1}^{n} \widetilde{\widetilde{\ell}}_s \sum_{\vec{m} \in \{1,\ldots4\}^n} \frac{(-1)^{\sum_{1 \leqslant s' < s'' \leqslant n} m_{s'} m_{s''} \tau(s', s'')}}{4^n}. \quad (25)$$

The expression $(-1)^{m_{s'} m_{s''} \tau(s', s'')}$ is invariant under shifting $m_{s'} \to m_{s'} + 2$ or $m_{s''} \to m_{s''} + 2$. Therefore, the sum over $\vec{m} \in \{1, \ldots, 4\}^n$ contains 2^n classes of 2^n equivalent configurations. Also, $m_j = 0$ is equivalent with $m_j = 2$. We conclude that the average position distribution of the Ising quantum walk after t steps, $\langle\langle p^{(\text{Ising})}(s,t) \rangle\rangle$, is given by (5) with average fusion space trace

$$\left\langle\left\langle \text{tr}\mathcal{Y}_{\bar{a}\bar{a}'}^{(\text{Ising})} \right\rangle\right\rangle = \left[\prod_{s=1}^{n} \widetilde{\widetilde{\ell}}_s \right] \mathcal{T}_{\bar{a}\bar{a}'}. \quad (26)$$

Here

$$\mathcal{T}_{\bar{a}\bar{a}'} = \frac{1}{2^n} \sum_{\vec{m} \in \{0,1\}^n} \prod_{1 \leqslant s' < s'' \leqslant n} (-1)^{m_r m_s \tau(s', s'')}, \quad (27)$$

which can be interpreted as an arithmetic mean of the quantity $(-1)^{\text{Arf}(L_{\bar{a}\bar{a}'}^*)}$ taken over all sublinks $L_{\bar{a}\bar{a}'}^*$ of a link $L_{\bar{a}\bar{a}'}$.

Note that while the Ising model anyons correspond to spin-1/2 irreps of the quantum group $SU(2)_2$, the braid generators for the two models are not identical. The primary difference relevant to our studies is the $R_{\frac{1}{2}\frac{1}{2}}$ matrix for braiding of two spin-1/2 irreps that fuse into spin-0 or spin-1 irreps. For Ising
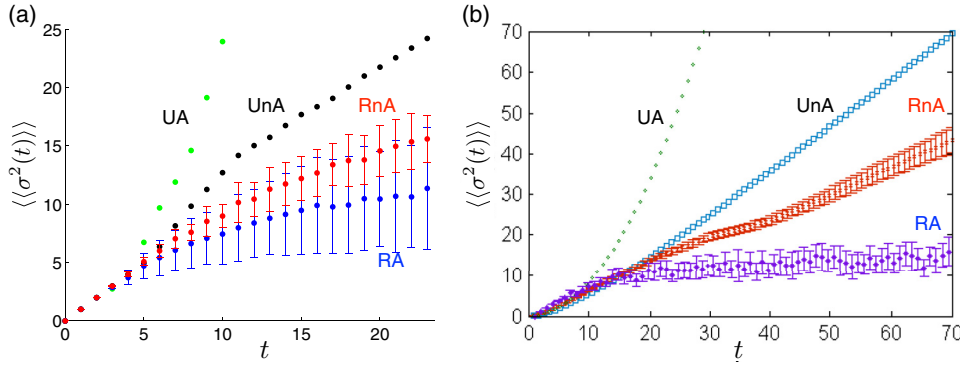
FIG. 6. (Color online) Numerical results for transport of Abelian and non-Abelian anyons. (a) Exact results for the discrete-time quantum walk with anyons over an $n = 46$ lattice. Here we plot the variances for Abelian anyons with $\frac{\pi}{8}$ exchange statistics around a uniform background of islands singly occupied by Abelian anyons (uniform Abelian, UA), Ising model anyons around a uniform background $m_s = 1 \, \forall \, s$ (uniform non-Abelian, UnA), Abelian anyons with the occupation probability uniform over $m_s \in \{0, \ldots, 7\}$ (random Abelian, RA; averaged over at least 100 configurations), and Ising anyons with $m_s \in \{1, \ldots, 4\}$ (random non-Abelian, RnA; 50 configurations). (b) Variance of anyons in a Hubbard model on a ladder realizing a continuous-time anyonic quantum walk over an $n = 100$ lattice. Here space and time axes are scaled so that a continuous-time classical diffusion would have a diffusion coefficient providing $\sigma^2(t) = t$. For the random non-Abelian model, island occupations are with $m_s \in \{0, \ldots, 4\}$ averaged over 50 configurations. The asymptotic slope for the RnA case is 0.54, and it remains positive and less than 1 within 1σ variance. Numerics are obtained using an approximate method employing real-time evolution of an anyonic MPS with the bond dimension equal to 100.

model anyons

$$R_{\text{Ising}}^{\frac{1}{2}, \frac{1}{2}} = e^{-i\frac{\pi}{8}} \begin{pmatrix} 1 & 0 \\ 0 & i \end{pmatrix}$$

and $R_{SU(2)_2}^{\frac{1}{2}, \frac{1}{2}} = i R_{\text{Ising}}^{*\frac{1}{2}, \frac{1}{2}}$. This implies the relevant braid generators for these models are equivalent up to a phase i and complex conjugation. In disordered walks, the distribution of stationary anyons is nonuniform, and the walker may thus pick up nontrivial phases from bra and ket evolution. The difference between these phases is given by the writhe w, which is the difference between positive and negative crossings in the link diagram. The total phase difference is then $i^w = i^{2\sum_{s=1}^{N} m_s \ell_s}$. However, in view of (18), the trace is zero unless ℓ_s is a multiple of 2, so that $i^w = 1$, and all the results herein hold equivalently for Ising and $SU(2)_2$ anyons.

A. Numerical calculations of non-Abelian anyons

We calculated the evolution numerically using two methods. First, the probability distribution was calculated exactly using Eqs. (4) and (22) up to 23 time steps, and the average variance $\langle\langle \sigma^{2(\text{Ising})}(t) \rangle\rangle$ over at least 100 charge configurations $m_s \in \{1, \ldots, 4\}$ was obtained [see Fig. 6(a)]. The average variance is approximately a straight line with slope of 0.456 from 10 to 23 time steps, but the error bars of the variance, obtained from the standard deviation, overlap with the error bars of the Abelian case, so we cannot distinguish between Abelian and non-Abelian anyons on this short time scale. Considering occupations $m_s \in \{0, \ldots, 4\}$ (vacuum charges included), the variance is slightly larger; that is, the wave packet is diffusing faster (not shown).

To obtain results for longer times, we turn to the continuous-time picture where the time evolution is generated by a Hubbard-type Hamiltonian H and the propagator $e^{-iH\delta t}$ implements an infinitesimal time evolution. The total Hamiltonian is given by the sum of the shift and coin flip terms

$H = H_{\text{shift}} + H_{\text{flip}}$, where [25]

$$H_{\text{shift}} = J \sum_s (T_{s+1}^- \hat{b}_s P_1 + T_s^+ \check{b}_s P_2) + \text{H.c.}, \quad (28)$$

$$H_{\text{flip}} = \sum_s (\kappa |2\rangle_s \langle 1| + \kappa^* |1\rangle_s \langle 2|), \quad (29)$$

where $J \in \mathbb{R}, \kappa \in \mathbb{C}$ and $T_s^{\pm} = (|1\rangle_{s\pm1 \, s}\langle 1| + |2\rangle_{s\pm1 \, s}\langle 2|) \otimes I_{\text{fusion}}$ are translation operators between sites s and $s \pm 1$, $\hat{b}_s$ are braid generators as defined above for braiding the mobile anyon around anyons in the island between s and $s + 1$ (acting on only fusion space), and $P_c = \sum_s |c\rangle_s \langle c| \otimes I_{\text{fusion}}$ are projectors to the coin states. Here $|c\rangle_s$ corresponds to occupation of state c at site s; that is, $|c = 0\rangle_s$ corresponds to the case with no mobile anyon at site s, and $|c = 1\rangle_s$ ($|c = 2\rangle_s$) is a mobile anyon with coin state $|0\rangle$ ($|1\rangle$) at site s. Here we consider only the case where coins are identical on every site.

The above Hamiltonian is the generator of continuous-time evolution for total time T. Running the continuous-time walk for time T simulates the discrete-time quantum walk in a stroboscopic manner, such that the walker makes $T/\delta t$ steps of infinitesimal length δt: $e^{-iHT} = (e^{-iH\delta t})^{T/\delta t}$. In the first order of Suzuki-Trotter expansion, the propagator decomposes to $e^{-iH_{\text{shift}}\delta t} e^{-iH_{\text{flip}}\delta t}$, similar to the single-step operator in the discrete-time quantum walk model.

We perform numerics on an $n = 100$ lattice with open (reflecting) boundaries using the "time-evolving block decimation" (TEBD) [26] algorithm that is based on matrix product states (MPS) using $J = \kappa = 1$ to mimic the discrete coin flip. Our implementation of the TEBD algorithm explicitly preserves anyonic charge and also particle number [27] corresponding to the presence of a single walker. Full details of the numerical simulation are given in Ref. [25]. Thus, while the position of the walker and the fusion degrees of freedom of the anyons are entangled during the time evolution, the algorithm preserves the distinction between them. This in turn allowed

for specification of total anyonic charge and particle number; here we consider the total vacuum sector with one walker. Figure 6 shows that for non-Abelian anyons the variance grows linearly as a function of time, indicating no signature of localization.

B. Correlations in time

The absence of localization in the non-Abelian case can be understood heuristically as a decoherence effect. The fusion Hilbert space $\mathcal{H}_{\text{fusion}}$ of the non-Abelian anyons acts as a nonlocal and highly non-Markovian environment whose dimension grows exponentially as $d^{|\vec{m}|}$. The entanglement between the quantum walk DOFs and fusion DOFs is known to erase the quantum effects in the case of uniform filling [8]. Furthermore, on comparing (26) to the Abelian expression (6) for $N = 8$, we find they are identical except for the prefactor $\mathcal{T}_{\bar{a}\bar{a}'}$. The key distinguishing feature is the decoherence introduced by this factor. Considering Eq. (6) to be the coherent expression where the quantum interference of probability amplitudes causes localization, we argue that the $\mathcal{T}_{\bar{a}\bar{a}'}$ coefficient can be viewed as a noise term due to the dependence on the link invariant τ, which fluctuates as the length of braids increases.

As shown in Ref. [28], the quantum walk is diffusive in the presence of both temporal and spatial disorders; in other words, localization does not occur in a spatially disordered system if temporal randomness is also present. The effect of $\mathcal{T}_{\bar{a}\bar{a}'}$ is that it multiplies the contribution from each path by the configuration average over $(-1)^{\sum_{1 \leqslant s' < s'' \leqslant n} m_{s'} m_{s''} \tau(s', s'')}$. While this term preserves the memory of the whole history of the particle's trajectory, we argue that at short time scales it fluctuates in a disordered manner. The value of τ changes when a new Borromean ring is formed, which requires at least four time steps. Also, the formation of a Borromean ring requires a very specific pattern in the particle's trajectory, which is in no way periodic. In addition, because of the condition on the last coin outcomes $a_t = a_t'$, there are new path patterns up to $t - 1$ time steps introduced in every time step which were not allowed for the previous time step, so these paths are not correlated to the previous evolution at all.

The time correlations of the τ invariant can be tracked by defining the correlator

$$C(t,t') = \frac{\langle (-1)^{\tau_t}(-1)^{\tau_{t-t'}} \rangle - \langle (-1)^{\tau_t} \rangle \langle (-1)^{\tau_{t-t'}} \rangle}{1 - \langle (-1)^{\tau_t} \rangle^2}, \quad (30)$$

where $\tau_t = \sum_{1 \leqslant s' < s'' \leqslant n} \tau(s', s'')$ is the sum of three-component invariants for all sublinks for a path up to t time steps and $\langle \cdot \rangle_{(\bar{a}, \bar{a}') \rightsquigarrow s_0}$ is the expectation value over all paths leading to the initial site s_0 (the subindex has been suppressed above for clarity). The term in the denominator is a normalization factor, which is defined to be the value of the term in the numerator in the perfectly correlated case $t' = 0$. For simplicity, the correlator is calculated for only the uniform filling ($m_s = 1 \, \forall s$) using the same method as described in [8]. The time correlations can be analyzed by keeping the final time t fixed and calculating the correlator for increasing values of t'. The intermediate time value $\tau_{t-t'}$ is calculated by erasing the t' last braid generators from the total braid word, such that braiding is switched off after $t - t'$ time steps. For some braid words, the quantity $\tau(s', s'')$ is not well
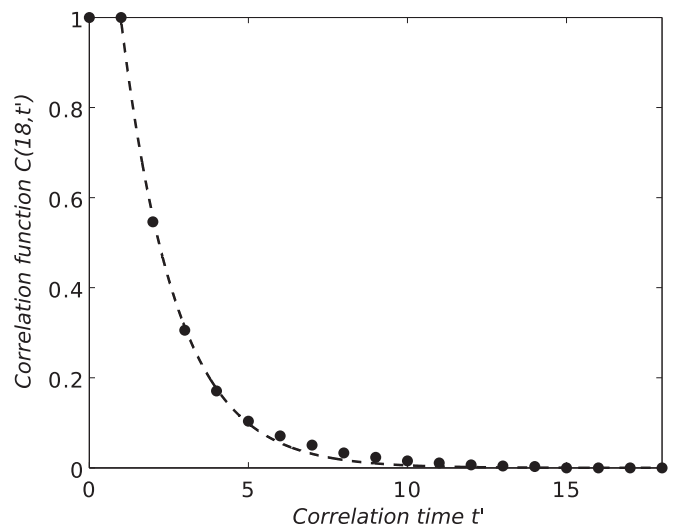

FIG. 7. Correlator $C(t,t')$ as a function of t' with the total number of time steps $t = 18$. The line shows the best exponential fit $C(18,t') = 1.77 \, e^{-0.58 \, t'}$. The value $C(18, t' = 18) \sim 10^{-16}$.

defined in our method, in which case we set $\tau(s', s'') = 0$. The correlator for $t = 18$ is plotted in Fig. 7, which shows that the correlations fall off exponentially after one step, indicating that, effectively, the τ invariant maintains memory only for a short period of time and the environment is Markovian at long time scales. Note that because of the condition $a_t = a_t'$, the braiding at the last time step can always be trivially undone; therefore the last two time steps are perfectly correlated. The correlator can also be calculated for other sites $s \neq s_0$. In these cases, the rapid falloff is observed for the central region $s_0 - t/\sqrt{2} \leqslant s \leqslant s_0 + t/\sqrt{2}$, and outside this region the falloff becomes linear at the farthest edge sites. The edge behavior is, however, irrelevant, as the behavior of the quantum walk is determined by the central region only.

The fundamental reason for the classical-like behavior of the walker is the strong entanglement between the quantum walk states and the fusion states, and the highly mixing nature of the fusion space environment. The walker states stay entangled with the fusion states for long time periods, and recurrences where these states become uncoupled happen very rarely.

We have also investigated the effect of temporally random phases introduced in the spatially random Abelian walk. In this model the wave function is multiplied by a random -1 phase with some probability p_{phase} if the walker crosses a site belonging to the temporally fluctuating region of sites. The calculations with different values of p_{phase} and different sizes of the region up to 500 time steps showed that the behavior becomes diffusive in all these cases.

V. CONCLUSIONS

An experimental demonstration of the disordered anyonic quantum walk could be realized with a chain of quantum double-point contacts in FQH liquids, as discussed in some detail in Ref. [29]. In that work the walker particle is a mobile edge excitation of the two-dimensional FQH liquid, coin mixing is achieved by (weak) tunneling between two

edges, and island populations can be changed by creating bulk excitations via top gates. The conductivity between the injection point and the measurement point is proportional to the probability to reach the absorbing boundary when the walker starts out by being localized at the injection point. Experimental control of such double-point contact devices and the observation of interference between fractional charges were reported in Refs. [30,31].

Our study provides a paradigm of disorder that has the ability to override the localization properties of quasiparticles with anyonic statistics. In a real system with random potentials Abelian anyons that do not localize due to the potentials can be localized just by the presence of a random anyonic environment. On the other hand, non-Abelian $SU(2)_2$ anyons that would localize due to some random potential can be delocalized if a random background of non-Abelian anyons is present.

We expect delocalization to occur even for more general $SU(2)_k$ non-Abelian anyons due to the entanglement of the walker with the environment. Indeed, it has been demonstrated that the entanglement of the walker with its uniform environment for any $k > 1$ is strong enough to cause the walk to decohere, eventually leading to a classical diffusive behavior [9].

APPENDIX: LOCALIZATION LENGTHS

1. Bounding the localization length

Here we compute the bounds on the localization length for Abelian anyons with exchange statistics π/N. This is done by computing $\langle\langle \ln |t_{1,n}|^2 \rangle\rangle$, which is the statistical average of the logarithm of the transition probability amplitude taken over the angles $\theta_1, \theta_2, \ldots, \theta_{n-1}$, which are valued in the discrete set $\{\frac{\pi}{N}m \mid m = 0, \ldots, N - 1\}$. To proceed, we carry out the θ_{n-1} average in the last term of (11),

$$\sum_{m_{n-1}=0}^{N-1} \frac{1}{N} \ln |1 - r_n r'_{1,n-1} e^{i\frac{2\pi}{N}m_{n-1}}|^2$$

$$= \frac{1}{N} \ln \left| \prod_{m_{n-1}=0}^{N-1} \left(1 - r_n r'_{1,n-1} e^{i\frac{2\pi}{N}m_{n-1}}\right) \right|^2$$

$$= \frac{1}{N} \ln |1 - (r_n r'_{1,n-1})^N|^2. \tag{A1}$$

In the latter equality we used the fact that

$$\prod_{m=0}^{N-1} \left(1 - C e^{i\frac{2\pi}{N}m}\right) = 1 - C^N, \tag{A2}$$

which can be proven by using Newton's identities between elementary symmetric polynomials and power sums [32].

The $\theta_1, \ldots, \theta_{n-2}$ average of (A1) becomes trivial once we estimate ($|r'_{1,n-1}| \leqslant 1$)

$$\ln[1 - (|r_n||r'_{1,n-1}|)^N]^2 \leqslant \ln |1 - (r_n r'_{1,n-1})^N|^2$$
$$\leqslant \ln[1 + (|r_n||r'_{1,n-1}|)^N]^2, \tag{A3}$$

$$\ln(1 - |r_n|^N)^2 \leqslant \ln |1 - (r_n r'_{1,n-1})^N|^2$$
$$\leqslant \ln(1 + |r_n|^N)^2. \tag{A4}$$

The upper and lower bounds of relation (11) read

$$\langle\langle \ln |t_{1,n}|^2 \rangle\rangle \leqslant \langle\langle \ln |t_{1,n-1}|^2 \rangle\rangle + \ln |t_n|^2 - \frac{1}{N} \ln(1 - |r_n|^N)^2 \tag{A5}$$

and

$$\langle\langle \ln |t_{1,n}|^2 \rangle\rangle \geqslant \langle\langle \ln |t_{1,n-1}|^2 \rangle\rangle + \ln |t_n|^2 - \frac{1}{N} \ln(1 + |r_n|^N)^2, \tag{A6}$$

respectively. When applied repeatedly, these recurrences yield $(t_{1,1} \equiv t_1)$

$$\langle\langle \ln |t_{1,n}|^2 \rangle\rangle \leqslant \sum_{j=1}^{n} \ln |t_j|^2 - \frac{1}{N} \sum_{j=2}^{n} \ln(1 - |r_j|^N)^2, \tag{A7}$$

$$\langle\langle \ln |t_{1,n}|^2 \rangle\rangle \geqslant \sum_{j=1}^{n} \ln |t_j|^2 - \frac{1}{N} \sum_{j=2}^{n} \ln(1 + |r_j|^N)^2,$$

where we have omitted the lower index of the averaging brackets $\langle\langle \cdots \rangle\rangle$.

2. Island distributions including N anyons each with exchange statistics $\frac{\pi}{N}$

The argument in the main text assumed anyon occupancies m_j in each of the islands were identically distributed independent random variables drawn from a uniform distribution over the set $\{m = 0, \ldots, N - 1\}$. If, instead, we expand the set to $\{m = 0, \ldots, N\}$ so that we can include populations having cumulative fermionic exchange phases with the walker, then the results do not change much. Using a similar analysis, one finds that the localization length satisfies the bounds

$$\xi_{loc}^{LB}(N) \leqslant \xi_{loc} \leqslant \xi_{loc}^{UB}(N), \tag{A8}$$

where

$$\xi_{\mathrm{loc}}^{UB}(N) = \frac{1}{\ln[(1-|r|^2)(1-|r|^N)]^{\frac{2}{N+1}} - \ln|t|^2},$$

$$\xi_{\mathrm{loc}}^{LB}(N) = \begin{cases} \frac{1}{\ln[(1+|r|^2)^2(|r|^{2N}+2|r|^N+1)]^{\frac{1}{N+1}} - \ln|t|^2}, & N \text{ odd}, \\ \frac{1}{\ln[(1+|r|^2+2|r|\cos\frac{\pi}{N})(|r|^{2N}+2|r|^N+1)]^{\frac{1}{N+1}} - \ln|t|^2}, & N \text{ even}. \end{cases} \quad (A9)$$

Again, these bounds are valid only for $N > 2$. Choosing, as before,

$$t = -\frac{1}{\sqrt{2}}, \quad t' = \frac{1}{\sqrt{2}}, \quad r = \frac{1}{\sqrt{2}}, \quad r' = \frac{1}{\sqrt{2}}, \quad (A10)$$

the localization length estimate for $N = 8$ ($\frac{\pi}{8}$ anyons) now has looser bounds,

$$1.218 \leqslant \xi_{\mathrm{loc}} \leqslant 1.906. \quad (A11)$$

Of course, in the limit $N \to \infty$, we have $\xi_{\mathrm{loc}} \to -\frac{1}{\ln|t|^2}$.

[1] J. M. Leinaas and J. Myrheim, Nuovo Cimento Soc. Ital. Fis. B **37**, 1 (1977).

[2] J. K. Pachos, *Introduction to Topological Quantum Computation* (Cambridge University Press, Cambridge, 2012).

[3] I. P. Radu, J. B. Miller, C. M. Marcus, M. A. Kastner, L. N. Pfeiffer, and K. W. West, Science **320**, 899 (2008); R. L. Willett, L. N. Pfeiffer, and K. W. West, Proc. Natl. Acad. Sci. USA **106**, 8853 (2009).

[4] V. Mourik, K. Zuo, S. M. Frolov, S. R. Plissard, E. P. A. M. Bakkers, and L. P. Kouwenhoven, Science **336**, 1003 (2012).

[5] M. H. Freedman, A. Kitaev, M. J. Larsen, and Z. Wang, Bull. Am. Math. Soc. **40**, 31 (2002).

[6] G. K. Brennen, D. Ellinas, V. Kendon, J. K. Pachos, I. Tsohantjis, and Z. Wang, Ann. Phys. (NY) **325**, 664 (2010).

[7] A. Ambainis, E. Bach, A. Nayak, A. Vishwanath, and J. Watrous, in *Proceedings of the 33rd Annual ACM Symposium on Theory of Computing* (Association for Computing Machinery, New York, 2001), pp. 37–49; A. Nayak and A. Vishwanath, arXiv:quant-ph/0010117.

[8] L. Lehman, V. Zatloukal, G. K. Brennen, J. K. Pachos, and Z. Wang, Phys. Rev. Lett. **106**, 230404 (2011).

[9] L. Lehman, D. Ellinas, and G. K. Brennen, J. Comput. Theor. Nanosci. **10**, 1634 (2013);

[10] P. W. Anderson, Phys. Rev. **109**, 1492 (1958).

[11] C. A. Müller and D. Delande, in *Les Houches 2009 - Session XCI: Ultracold Gases and Quantum Information*, edited by C. Miniatura *et al.* (Oxford University Press, Oxford, 2011), Chap. 9.

[12] Allowing for total island charge that is fermionic, i.e., $m_j \in \{0, \ldots, N\}$, does not change the results much (see Appendix A2).

[13] V. Zatloukal, M.S. thesis, Czech Technical University in Prague, 2011; http://ssmf.fjfi.cvut.cz/2008.html.

[14] F. Klopp and K. Pankrashkin, Lett. Math. Phys. **87**, 99 (2009).

[15] J. T. Chalker and S. Siak, J. Phys.: Condens Matter **2**, 2671 (1990).

[16] H. Schanz and U. Smilansky, Phys. Rev. Lett. **84**, 1427 (2000).

[17] X. Chen, L. Fidkowski, and A. Vishwanath, Phys. Rev. B **89**, 165132 (2014).

[18] L. H. Kauffman, Topology **26**, 395 (1987).

[19] D. Aharonov, V. Jones, and Z. Landau, Algorithmica **55**, 395 (2009).

[20] V. F. R. Jones, Bull. Am. Math. Soc. **12**, 103 (1985).

[21] H. Murakami, Math Semin. Notes **11**, 335 (1983).

[22] R. Kirby and P. Melvin, Geom. Topol. Monogr. **7**, 213 (2004).

[23] If we include the vacuum island occupation and consider a model with $W(m) = 1/5$ for $0 \leqslant m \leqslant 4$, numerics show that the variance of the resulting walker's position distribution grows even faster.

[24] Recall that $\tau(s', s'')$ can be nonzero only if $\ell_{s'}, \ell_{s''} = 0$.

[25] S. Singh, R. N. C. Pfeifer, G. Vidal, and G. K. Brennen, Phys. Rev. B **89**, 075112 (2014).

[26] G. Vidal, Phys. Rev. Lett. **93**, 040502 (2004).

[27] S. Singh, R. N. C. Pfeifer, and G. Vidal, Phys. Rev. B **83**, 115125 (2011).

[28] A. Albrecht, C. Cedzich, R. Matjeschk, V. B. Scholz, A. H. Werner, and R. F. Werner, Quantum Inf. Process. **11**, 1219 (2012).

[29] V. Zatloukal, L. J. Lehman, J. K. Pachos, and G. K. Brennen, Quantum Comput. Comput. **12**, 51 (2012).

[30] R. L. Willett, L. N. Pfeiffer, and K. W. West, Proc. Natl. Acad. Sci. USA **106**, 8853 (2009).

[31] R. L. Willett, L. N. Pfeiffer, and K. W. West, Phys. Rev. B **82**, 205301 (2010).

[32] I. G. Macdonald, *Symmetric Functions and Hall Polynomials*, 2nd ed. (Clarendon, Oxford, 1995).